Electrochemical switching of the Peierls-like transition in metallic single-walled carbon nanotubes

Peter M. Rafailov,* Janina Maultzsch, and Christian Thomsen
Institut für Festkörperphysik, Technische Universität Berlin, Hardenbergstr. 36, 10623 Berlin, Germany

Hiromichi Kataura
Nanotechnology Research Institute (NRI), National Institute of Advanced Industrial Science and Technology (AIST), Central 4, Higashi 1-1-1, Tsukuba, Ibaraki 305-8562, Japan

(Received 15 December 2004; revised manuscript received 14 April 2005; published 7 July 2005)

The high-energy vibrational modes of metallic carbon nanotubes are believed to be softened compared to the semiconducting ones by a Peierls-like transition. The Raman modes, when excited with a red laser to enhance the metallic tubes, were found to exhibit an exceptionally high sensitivity to electrochemical doping. Our data may be interpreted as controlling the Peierls-like instability in metallic tubes with the applied potential. We also discuss the limits of applicability of the double-layer charging model and show Raman evidence for a hysteretic transition to a chemical doping regime.

DOI: 10.1103/PhysRevB.72.045411 PACS number(s): 78.30.Na, 63.22.+m, 82.45.Yz

I. INTRODUCTION

Single-walled carbon nanotubes (SWNT) are promising nanostructures with remarkable properties that are important for both fundamental science and device applications. SWNTs possess an electronic structure with a markedly one-dimensional character,[1,2] large surface-to-volume ratio, good chemical stability and significant elastic properties;[3] thus appearing as appropriate candidates for supercapacitors,[4] batteries,[5] actuators,[6] and various electronic devices. For instance, the change in resistivity of a semiconducting SWNT by many orders of magnitude upon electrostatic gating or gas absorption has a potential for applications, such as SWNT-FETs (field-effect transistors)[7] or electrochemical sensors.[8] Plenty of the mentioned applications are related to doping of SWNTs as their electronic and mechanical properties are very sensitive to charge transfer. This sensitivity, on the other hand, makes Raman spectroscopy a powerful and favored tool to examine doping-induced phenomena.

There are several ways to dope carbon nanotubes. A high degree of charge transfer can be achieved by intercalation. The intercalation of SWNT with alkali metals,[9,10] I (Ref. 11) and Br (Ref. 9) was studied in detail by Vis-IR (Ref. 10) and Raman[9,11] spectroscopy and x-ray diffraction.[11,12] During intercalation the guest species move into the interstitial channels of the SWNT ropes and form a stable charge-transfer compound.[11] The penetration of the intercalant into the SWNT rope channels has been established by x-ray diffraction,[12] directly, and by Raman spectroscopy showing a strong shift of the radial breathing mode[9] (RBM) and a shift accompanied by a change in spectral shape of the high-energy band[9,13–15] upon intercalation.

Alternatively, the electronic structure of SWNTs can be changed electrochemically by varying the potential at their contact interface with an electrolytic solution.[6,16] Vis-NIR and Raman studies combined with this approach[16–18] show that finer tuning of the added charge can be accomplished. However, the achievable doping level is lower, since the electrolyte ions do not readily penetrate the SWNT ropes. Instead, during the initial stages of electrochemical doping, they form a charged double layer only with the external surface of the ropes.[17,19,20] This is of key importance for the SWNT application as actuators because SWNT expansion or contraction can be related to the transferred charge, which in the double-layer model can be calculated from the applied voltage. This is possible because of the good contact of the outer surface of SWNT bundles with the electrolytic solution, the linear scaling of the phonon frequency with the applied voltage,[17,20] and its proven independence of the electrolyte used.[20]

The behavior of the high-energy SWNT mode (HEM) upon doping in an electrolytic solution has been intensively studied[17,18,20] at the most common laser excitation of 2.41 eV, and the mode was found to shift by $\approx 250\ \mathrm{cm}^{-1}/\mathrm{hole/C\text{-}atom}$ ($\approx 1.5\ \mathrm{cm}^{-1}/\mathrm{V}$). From this doping-induced frequency shift useful information on the SWNT actuation properties can be obtained.[20,21] Interesting observations were also made for excitation energies at which metallic SWNTs are resonant: these lie typically in the 2.2–1.7 eV region for the most commonly used nanotubes (diameters 1.1–1.5 nm). In this "metallic resonance window" doping successively restores the HEM shape characteristic for semiconducting SWNTs, causing the broad "metallic" band at the low-frequency side of the HEM to vanish.[14,18,22] This effect was attributed to a depletion of charge carriers from the valence-conduction bands that participate in the first resonant optical transition in metallic SWNTs.[22] Such an explanation, however, assumes that electrochemical doping yields doping levels comparable to those of intercalation (up to ≈ 0.1 holes/C-atom) which are able to deplete the first metallic transition at ≈ 1.9 eV.

The HEM phonon softening in metallic nanotubes was explained recently by a Peierls-like mechanism.[23] One prerequisite for this mechanism to be effective is the valence-conduction band crossing right at the Fermi wave vector k_F. This would imply that even a small external influence shift-

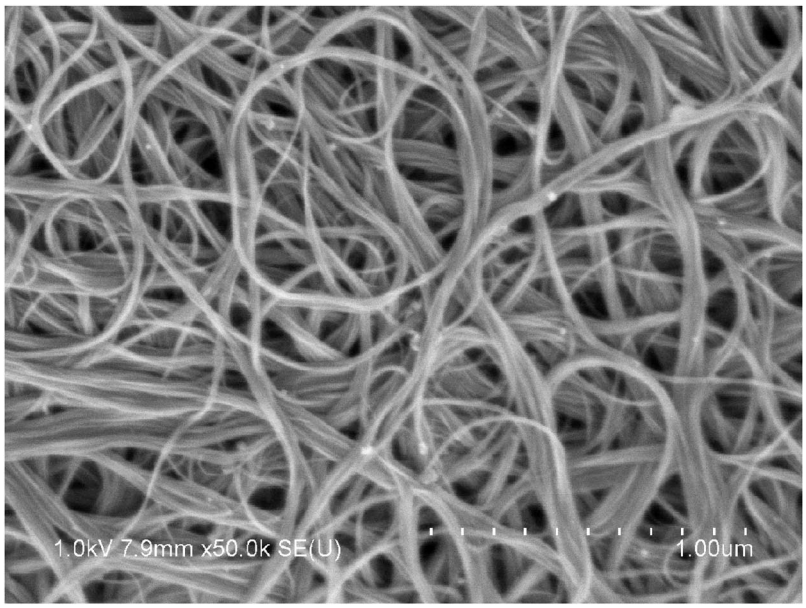

FIG. 1. SEM image of the investigated SWNT bundles

ing the crossing point in the hexagonal plane away from k_F, should be able to weaken the softening mechanism. Here we report a resonant Raman investigation of SWNTs exposed to both *p*- and *n*-type electrochemical doping under strictly defined double-layer conditions. We establish a strong hardening of the HEM phonons of metallic SWNTs upon charge injection of either sign at very low doping levels, which is consistent with a possible removal of a Peierls-like instability. Our results thus lend support to the explanation of the phonon softening in metallic tubes by a Peierls-like mechanism.

II. EXPERIMENTAL

The carbon nanotubes used in this work were grown by the laser ablation method. This method can control precisely the diameter distribution of SWCNTs for a wide range[24] from 0.7 to 1.6 nm. We used SWCNTs with mean diameter at 1.4 ± 0.1 nm prepared using NiCo catalyst in 1250 C Ar gas. The diameter distribution was confirmed by Raman spectrum and x-ray-diffraction (XRD) analysis.

Typically, the raw soot obtained after laser ablation contains 60% SWNTs, 30% amorphous carbon, and 10% fullerenes. We removed fullerenes by heating in vacuum to 650 °C. The soot was refluxed in a 15% H_2O_2/water solution at 100 °C for 3 h. Active oxygen burned out amorphous-carbon particles at 100 °C. The remaining metal particles were washed out by sonication in HCl-water solution. The purified SWNTs were formed into thin black paper by simple filtration and then dried in vacuum at 650 °C. Very thin and porous SWNT mats were obtained in this way, with a purity higher than 90% as determined by TEM observations. Figure 1 shows a typical scanning electron microscopy (SEM) image of the SWNT paper.

Stripes of ~1 mm width and 10 mm length of the as obtained SWNT mats were prepared as working electrodes in a three-electrode cell equipped with quartz windows. The measurements were carried out using a Metrohm Three-Electrode-Potentiostat. A platinum wire and Ag/AgCl/3 M KCl served as auxiliary and reference electrode, respectively. The working electrode was partly dipped into the solution (1 M aqueous solution of NH_4Cl) and was electrically contacted by means of silver paint at its dry end. The double-layer capacitance of the working electrode was measured by cyclic voltammetry[20] and found to be $C \approx 35$ F/g. The electrolyte solution was purged with N_2 gas prior to measurements to remove excessive oxygen. All chemicals used were of analytical grade quality. The solutions were prepared using doubly destilled water. An Ar^+/Kr^+ laser (2.41 eV) and a dye laser (1.95 eV) were used for excitation. The Raman spectra were recorded with a DILOR triple grating spectrometer equipped with a charge-coupled device (CCD) detector. The spectrometer was calibrated in frequency using a Neon lamp and the laser plasma lines.

III. RESULTS AND DISCUSSION

A. Some details of the double-layer regime

In our previous work we described Raman measurements on electrochemically doped samples of the same buckypaper in various alkali metal salt solutions. The Raman spectra measured in different solutions at the same applied potential did not exhibit any anion- or cation-specific differences.[20] After comprehensive tests of our experimental conditions, as described in Ref. 20, we were able to prove that double-layer charging is the main doping mechanism in the region from −200 mV to 1 V without a significant penetration of ionic species into the nanotube bundles. Additional support for the double-layer model in this potential window comes from the fact that the measured capacitance C is independent of the particular electrolyte used, and the frequency shift of the main HEM peak (≈ 1590 cm^{-1}) scales linearly with the applied potential U. The latter can be used to estimate the SWNT actuation properties (strain versus transferred charge),[20] as the transferred charge $Q = CU$. At higher nega-

tive potentials we cannot exclude an alkali cation diffusion into the bundles, given that the ionic diameter even of K^+ (0.28 nm) is smaller than the distance between neighboring walls of SWNTs in a bundle. Such a diffusion would comprise an intercalation onset in addition to the double-layer charging. Indeed, with Li doping it is possible to electrochemically intercalate the interior spaces of SWNTs.[25] In the present study we extended our experiments to almost the whole region of stability of water (±1 V) by using NH_4Cl as electrolyte, utilizing the larger ionic diameter of the NH_4 cation. Although the hydratized ionic diameters of NH_4^+ and K^+ are nearly the same, the larger size of NH_4^+ may more effectively prevent its massive penetration into the interstitial channels of the SWNT bundles at higher negative potentials.

The doping level f can be estimated as[17]

$$f = M_C CU/F, \tag{1}$$

where M_C is the atomic weight of carbon, U is the applied potential, and F is the Faraday constant. For our working electrode this yields a doping level that does not exceed 0.005 e^-(holes)/C-atom/V. Note that this kind of charge injection creates much lower doping levels than does, for example, intercalation.

We recorded Raman spectra of the high-energy mode from the SWNT working electrode at different constant potentials between −950 and 1060 mV (all potentials quoted were measured versus Ag/AgCl and corrected for the open circuit potential of 210 mV). All spectra could be well fitted by four Voigt profiles centered at about 1587, 1560, 1542, and 1520 cm^{-1} (shown with the lowest trace in Fig. 2(a)). Hereafter these four lines will be referred to as P1, P2, P3, and P4, implying that each peak actually corresponds to an ensemble of lines because of the variety of chiralities and diameters in our sample. P3 and P4 consist of bond-stretching modes of metallic SWNTs that are known to be resonant at red excitation.

B. Experimental results

The Raman spectra for several constant potentials at an excitation energy of 1.95 eV are displayed in Fig. 2(a). The fitted peak frequencies are plotted as a function of the applied potential in Fig. 2(b) for P1 and 2(c) for P3 and P4, respectively. Within the interval from −900 to 900 mV, the frequency of P1 shifts linearly with doping with slightly different slopes for positive and negative voltages of $\sim 1-1.5$ cm^{-1}/V. This fits well into what is known for this peak that dominates the HEM: a linear frequency shift that is largely independent of the excitation energy.[26,27]

In contrast, P3 and P4 exhibit a strong hardening upon doping of either sign: ~6 cm^{-1} and 8 cm^{-1} in going to −1 and 1 V, respectively. An important feature of this hardening is its nonlinearity and an apparent dramatic loss of intensity with increasing doping level. A similar effect was reported in Refs. 18 and 22 where the observed shift of the metallic modes was even 11 cm^{-1}. Corio *et al.*[22] explain the shift and the intensity decrease of these modes assuming that the doping level for applied potentials above 0.6 V becomes sufficiently high for the Fermi level E_F to pass through one of the

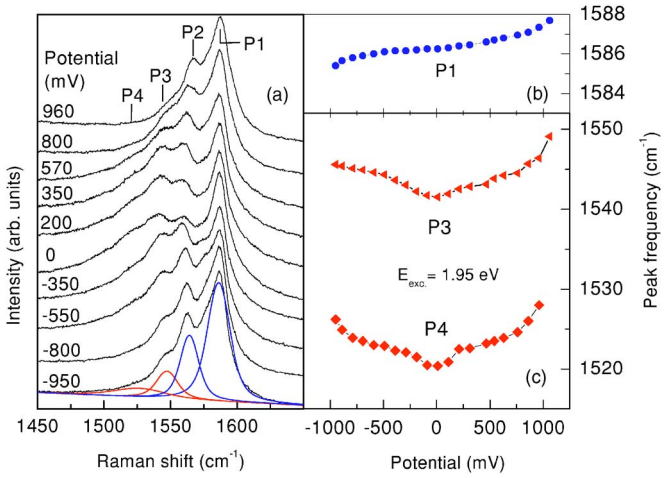

FIG. 2. (Color online) (a) Raman spectra at 1.95 eV excitation energy of the high-energy mode (HEM) at several potentials applied to the SWNT electrode in 1 M NH_4Cl aqueous solution. (b) The frequency of the main HEM peak P1 as a function of the applied potential (circles, blue). (c) Same as (b) for the peaks P3 (triangles, red) and P4 (diamonds, red).

mirror-imaged van Hove singularity governing the first optical transition of metallic SWNTs at ≈1.9 eV. However, E_F shifts of the order 1 eV are only achievable upon heavy doping as, e.g., chemical intercalation provides. Here we propose a crude estimate of the Fermi level shift upon electrochemical doping with applied potentials ~1 V ($f \approx 0.005$) based on optical absorption results[10,17] and *ab initio* calculations.[28,29]

C. Comparison to optical experiments and conclusions

Optical absorption measurements on SWNTs established three bands at about 0.68, 1.2, and 1.8 eV arising from the first and second optical transition in semiconducting tubes and the first optical transition in metallic tubes, respectively. The behavior of these bands upon charge injection was examined with both chemical and electrochemical doping. Extensive studies with both donor- and acceptor-type chemical doping were done by Kazaoui *et al.*[10] In the initial doping stages (typically $0 \leqslant |f| \leqslant 0.005$) they observed an intensity decrease for the absorption band at 0.68 eV without a change in the features at 1.2 and 1.8 eV. Subsequent doping (up to $f=0.04$) led to a large depletion of both bands at 0.68 and 1.2 eV without a change in the band at 1.8 eV. Optical absorption in electrochemically doped SWNTs was measured by several research groups on various kinds of samples and in different electrolyte media.[16,17,30] However, in all these experiments the model of double-layer charging of SWNT bundles can be applied. The results reported show that up to ≈0.5 V applied potential the three bands largely preserve their intensity. In the course of further potential increase the 0.68 eV band progressively diminishes, and at 1 V little or no intensity remains. The band at 1.2 eV starts diminishing in the vicinity of 1 V but at 1 V it still has most of its intensity; between 1 and 1.2 V it then quickly disappears. The band at 1.8 eV remains largely unaffected up to 1 V.

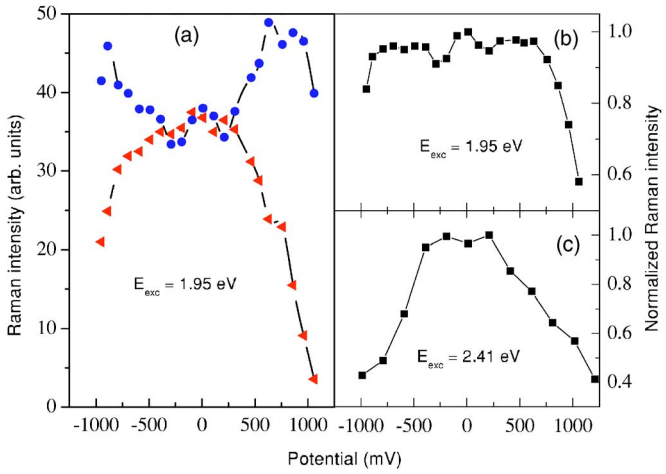

FIG. 3. (Color online) (a) Integrated Raman intensity of the peaks P3+P4 of metallic SWNTs (triangles, red) and P1+P2 (circles, blue) of the high-energy band as a function of the applied potential. See text and Fig. 1 for explanation on the peak notations. (b) Total Raman intensity of the high-energy band with 1.95 eV excitation as a function of the applied potential. (c) Same as (b) for 2.41 eV excitation.

Beyond 1 V and especially above 1.2 V it also quickly disappears, possibly due to a change in the doping mechanism at high potentials. From these results it can be concluded that $f=0.005$ corresponds to a E_F shift ΔE_F of 0.3 to 0.6 eV.

There are several theoretical estimations of the Fermi level shift for chemical doping with alkali metals. Although these calculations were done for intercalative doping levels (typically $0.05 \leqslant f \leqslant 0.2$), we can make a crude estimate of the upper bound of ΔE_F by interpolating published data assuming a complete charge transfer from the donor atoms. We obtain $\Delta E_F \leqslant 0.3$ eV for Na intercalation as red from Fig. 4(d) of Ref. 28 and $\Delta E_F \leqslant 0.2$ eV and $\Delta E_F \leqslant 0.5$ eV for Li and K intercalation, respectively, from Fig. 3 of Ref. 29. This is consistent with the results of a recent combined experimental and theoretical study[31] which estimated a necessary charge transfer of 0.008 electron/C-atom to reach $\Delta E_F = -0.8$ eV.

It thus follows from both theoretical and experimental studies that the Fermi-level shift amounts to at least 0.3 eV but hardly surpasses 0.6 eV at $|f|=0.005$. Especially, the first metallic van Hove singularity (≈ 0.9 eV) is not reached and not depleted at $U=1$ V for the vast majority of metallic SWNTs in our sample. For even lower doping between 300 and 500 mV where the metallic modes in the Raman spectra are already undergoing sizable changes, we estimate ΔE_F between 0.1 and 0.2 eV.

Next we analyze the peak intensities in the high-energy mode. In Fig. 3(a) we plotted the Raman intensity of the metallic modes and the intensity sum of P1 and P2 that comprise what is known as the "semiconducting" HEM shape outside the metallic resonance region, as a function of the applied potential. As is nicely seen from Fig. 3(a), besides the expected diminishing of the P3+P4 intensity, there is actually a gain in the P1+P2 intensity as doping progresses. What appears to be a mere intensity loss of metallic modes can thus be viewed as a redistribution of Raman intensity within the HEM, the modes of metallic SWNTs moving under the envelope of the semiconducting HEM. An indication for similar redistribution can be found also in Figs. 2(a) and 2(b) of Ref. 22 when comparing the plots at $U=0$ V and $U=0.6$ V. For further confirmation we display the dependence of the total HEM intensity (P1+P2+P3+P4) on the applied potential in Fig. 3(b). The plot shows that there is almost no net loss in the HEM intensity between −900 mV and 900 mV, which approximately marks the limits of applicability of the double-layer charging model. An important note on the behavior of P2 should be made here. At blue or green excitation its reaction to electrochemical doping is quite similar to that of P1—it softens upon electron and hardens upon hole injection[20] at a rate of ≈ 1.5 cm$^{/1}$V. In the present spectra, however, P2 qualitatively follows the behavior of the metallic peaks P3 and P4 (see Fig. 3). We argue that this is a mimic effect from the metallic modes that move into P2 and pass through it upon increasing the potential, and therefore we leave P2 without consideration in the present discussion.

Combining the behavior of peak frequencies and Raman intensity of the metallic modes, it is important to note that both are strong and nonlinear effects that take place upon a relatively small doping ($0 \leqslant |f| \leqslant 0.005$). For comparison, the P1 shift, which reflects the mere phonon softening due to doping-induced change in the C-C bond stiffness, is linear and almost 10 times smaller than the shift of the metallic modes. The metallic modes thus behave like in a position of unstable equilibrium. That is why we consider this as an experimental confirmation for the theory of Dubay *et al.*[23] that the softening of metallic modes is due to a Peierls-like mechanism.

According to *ab initio* results of Dubay *et al.*[23] the longitudinal optical (LO) phonon modes of A_1 symmetry in metallic nanotubes strongly couple to the electronic states at the Fermi level when the system is half filled, i.e., the valence-conduction band crossing occurs exactly at E_F. The coupling leads to an opening of a temporary band gap with a size oscillating in unison with the displacement pattern of the A_1(LO) modes. The formation of this gap lowers the energy of the filled states thus reducing the energy required to distort a metallic nanotube. Since only Γ-point phonons exhibit this coupling and the phonon dispersion is continuous, a large drop of up to several tens of centimeters^{-1} in the energy of the LO branch toward the Γ point and a crossing with the (transversal optical) (TO) branch[32] in metallic SWNTs takes place, while away from the Γ-point the LO branch may still exhibit its normal overbending and remain largely unaffected.[33] The resulting HEM Raman spectrum was shown to originate from a double-resonance scattering:[34] In double resonance the phonon state to be excited is determined by a unique combination of incident photon energy and phonon wave vector, depending on the particular electronic and phonon dispersion. Our laser energy of 1.95 eV is slightly above the energy of the first optical transition of the majority of metallic SWNTs in our sample. Therefore the excited phonon states lie very near to the Γ point with softened frequencies as expected. The LO phonon states give rise to the metallic broadening of the HEM band (peaks P3 and P4). The TO states do not exhibit such a strong electron-

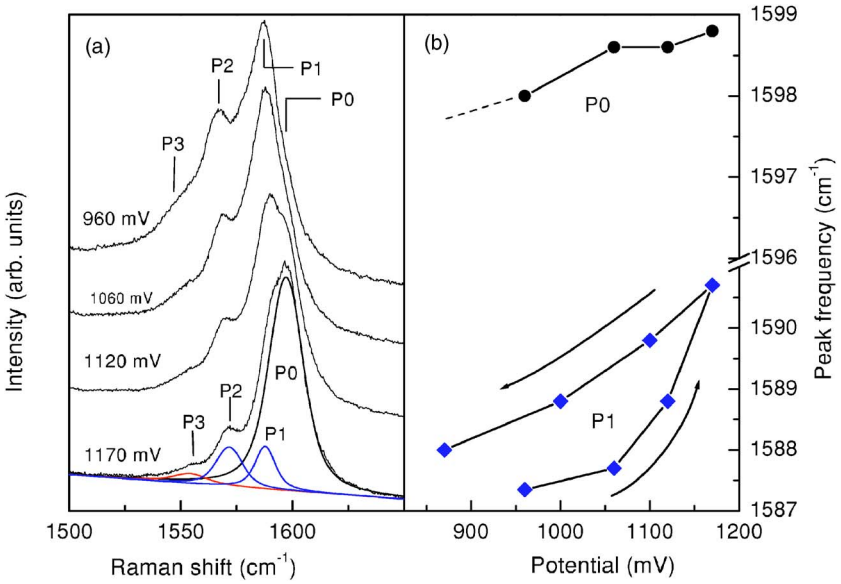

FIG. 4. (Color online) (a) Raman spectra at 1.95 eV excitation of the HEM upon electrochemical doping at several high potentials. (b) Measured frequencies of the peak P1 (diamonds, blue) and the newly appearing peak P0 (circles, black) at 1598 cm^{-1} as a function of the applied potential. Both arrows mark the sequence of increasing-releasing potential in the hysteresis of P1.

phonon coupling, and their scattering intensity should be lower without a drop in frequency. They presumably participate in the 1560–1590 cm^{-1} region of the HEM (peaks P1 and P2), where the Raman intensity of semiconducting SWNTs is concentrated.

Electrochemical doping of either sign quickly shifts the Fermi level away from the valence-conduction band crossing point, which should weaken the coupling of the metallic A_1(LO) phonons. Moreover, on approaching potentials of 1 V the E_F shift becomes comparable to the estimated amplitude 0.5 eV of the oscillating band gap[23] in the undoped state, thus, effectively hindering the gap opening. Therefore, our observation of metallic phonon hardening and intensity redistribution within the HEM upon electrochemical charging can be explained with removal of a Peierls-like instability that affects the phonon frequencies in the undoped state. In other words, applying a potential to metallic nanotubes can switch on or off their Peierls-like instability. The gathering of metallic modes under the envelope of a semiconducting-like HEM also supports the recent conclusion that a "semiconducting" HEM shape can originate from both semiconducting and metallic tubes.[33] When excited with a blue laser, phonon states with a larger wave vector are selected for the Raman process. In metallic tubes these states have higher frequencies in the same range as those of semiconducting tubes as the coupling leading to Peierls-like instability involves only Γ-point phonons. A red laser excitation combined with electrochemical doping that shifts the Γ-point LO states back to higher frequencies should therefore have the same effect as blue laser excitation, which is indeed observed experimentally.[33]

The fact that the total HEM intensity is largely preserved up to ≈900 mV [Fig. 3(b)] may indirectly be helpful for another issue. A large and progressive drop in the HEM intensity of electrochemically doped SWNTs has been established for excitation with 2.41 or 2.54 eV.[16,17,20] As a typical example in Fig. 3(c) we present the dependence of the total HEM intensity on the applied potential in such a Raman measurement (2.41 eV excitation). A sizable intensity drop is observed already at potentials as low as 400 mV with a particularly strong decreasing trend toward 1 V, where the intensity is ≈50% lower. The reason for this drop is still unclear, however, according to Ref. 17 it may be due to a depletion of the third optical transition in semiconducting SWNTs at ≈2.4 eV. Although this might be true for potentials fairly above 1 V, it is hardly possible below 1 V. Especially, before such a depletion can occur, the first metallic transition has to be depleted. A comparison between Figs. 3(b) and 3(c) clearly shows that below 1 V this is not the case.

D. Breakdown of the double-layer regime

All changes in the Raman spectra were found to be completely reversible for potentials up to 1 V, as is expected for a double-layer charging. In the following we demonstrate how the double-layer regime can be switched to a intercalative doping regime by further increasing the potential above 1 V. In Fig. 4(a) we present Raman spectra of the HEM taken in a sequence of measurements with increasing the potential to 1170 mV. The most striking feature in these spectra is a steep nonlinear hardening of all HEM constituents (peak P3 shifts above 1550 cm^{-1}) and the appearance of a new peak P0 at ≈1598 cm^{-1} on the high-frequency side of P1. This peak quickly gains intensity from P1 and becomes the most intense HEM peak at 1170 mV. This is accompanied by an exponential increase of the current in the electrochemical cell. Although it is negligible below 1 V, it reaches several hundred microamperes at at 1170 mV. In Fig. 4(b) we present the frequencies of P1 and P0 as a function of the applied potential. In addition to the nonlinear hardening of P1 in this potential range a hysteresis of frequency versus potential dependence is found, see Fig. 4(b). A hysteresis of P0 could not be established, as it is well shaped only at the highest measured potentials and the fitting precision is limited at lower potentials.

The observed effects at potentials above 1 V strongly indicate that a chemical reaction takes place between the work-

ing electrode and the electrolyte. The limit of stability of water is reached and the overvoltage of Cl on carbon is possibly compensated in this potential range, further complicating the doping mechanism. We give a tentative explanation of the observed hysteresis by pointing out that the Raman spectrum at 1170 mV in Fig. 4(a) is fairly similar to the Raman spectra of $SOCl_2$-functionalized SWNTs presented in Ref. 31. We argue that the most probable scenario at these high potentials is a breaking of the double layer, a penetration of Cl^- and newly formed Cl_2 into the SWNT bundles, and functionalization, i.e., adsorption of these chlorine species on the SWNT surface. Because of the direct charge transfer, in this case the doping level increases at a much higher rate than with double-layer charging as indicated by the nonlinear behavior and intensity decrease of the Raman peaks. A formation of C-Cl and C-O bonds, however, appears unlikely in view of the fact that a chlorination of multiwalled carbon nanotubes with a formation of covalent C-Cl bonds was only achieved after heavy electrolysis with a current as high as 100 mV applied for at least 16 h.[35]

The appearance of the new Raman peak P0 approximately coincides with the onset of the hysteresis [see Fig. 4(a)], which implies that P0 may come from Cl-functionalized SWNTs. Then, if our explanation of the hysteresis proves correct, it will be possible to follow the functionalization process with Raman spectroscopy by monitoring the development of the peak P0. Such a monitoring must, however, be done on fresh samples because our previous results[26] show that in multiply used samples P0 emerges at successively lower potentials, occuring even within the limits of the double-layer regime. Another unresolved issue is the excitation selectivity of P0:[26] it emerges only upon excitation in the metallic resonance window 1.7–2.2 eV. In Raman spectra excited with a blue, green, or infrared laser P0 is absent. Therefore, further studies are needed to completely clarify the origin of P0.

IV. CONCLUSIONS

We performed a Raman investigation of the high-energy modes of metallic SWNTs upon electrochemical doping. We found these modes to be extremely sensitive to quite low doping levels that is manifested in large frequency shifts and a dramatic intensity redistribution within the high-energy Raman band. We argue that these phenomena occur because of switching off the Peierls-like instability that governs the softening of the high-energy modes in metallic carbon nanotubes. We also present spectroscopic evidence for a transition from a low-doping regime governed by double-layer charging to hysteretic intercalative doping.

ACKNOWLEDGMENTS

We gratefully acknowledge W. Frenzel for his help with the electrochemical measurements. We thank M. Stoll for supplying us with some of the Raman spectra used in this study. This work was supported by the Deutsche Forschungsgemeinschaft under Grant No. Th 662/8-2. A part of this work was conducted in AIST Nano-Processing Facility, supported by "Nanotechnology Support Project" of the Ministry of Education, Culture, Sports, Science and Technology (MEXT), Japan.

*Electronic address: rafailov@physik.tu-berlin.de

[1] S. Reich, C. Thomsen, and J. Maultzsch, *Carbon Nanotubes: Basic Concepts and Physical Properties* (Wiley-VCH, Berlin, 2004).

[2] A. M. Rao, E. Richter, S. Bandow, B. Chase, P. C. Eklund, K. A. Williams, S. Fang, K. R. Subbaswamy, M. Menon, A. Thess, R. E. Smalley, G. Dresselhaus, and M. S. Dresselhaus, Science **275**, 187 (1997).

[3] C. Thomsen, S. Reich, H. Jantoljak, I. Loa, K. Syassen, M. Burghard, G. S. Duesberg, and S. Roth, Appl. Phys. A: Mater. Sci. Process. **69**, 309 (1999).

[4] C. Liu, A. J. Bard, F. Wudl, I. Weitz, and J. R. Heath, Electrochem. Solid-State Lett. **2**, 577 (1999).

[5] A. S. Claye, J. E. Fisher, C. B. Huffman, A. G. Rinzler, and R. E. Smalley, J. Electrochem. Soc. **147**, 2845 (2000).

[6] R. H. Baughman, C. Cui, A. Zakhidov, Z. Iqbal, J. N. Barisci, G. M. Spinks, G. G. Wallace, A. Mazzoldi, D. D. Rossi, A. G. Rinzler, O. Jaschinski, G. S. Roth, and M. Kertesz, Science **284**, 1340 (1999).

[7] S. J. Tans, A. Verschueren, and C. Dekker, Nature (London) **393**, 6680 (1998).

[8] A. Modi, N. Koratkar, E. Lass, B. Wei, and P. M. Ajayan, Nature (London) **424**, 171 (2003).

[9] A. M. Rao, P. C. Eklund, S. Bandow, A. Thess, and R. E. Smalley, Nature (London) **388**, 257 (1997).

[10] S. Kazaoui, N. Minami, R. Jacquemin, H. Kataura, and Y. Achiba, Phys. Rev. B **60**, 13339 (1999).

[11] L. Grigorian, K. A. Williams, S. Fang, G. U. Sumanasekera, A. L. Loper, E. C. Dickey, S. J. Pennycook, and P. C. Eklund, Phys. Rev. Lett. **80**, 5560 (1998).

[12] A. S. Claye, N. M. Nemes, A. Janossy, and J. E. Fisher, Phys. Rev. B **62**, R4845 (2000).

[13] N. Bendiab, L. Spina, A. Zahab, P. Poncharal, C. Marliere, J. L. Bantignies, E. Anglaret, and J. L. Sauvajol, Phys. Rev. B **63**, 153407 (2001).

[14] N. Bendiab, E. Anglaret, J. L. Bantignies, A. Zahab, J. L. Sauvajol, P. Petit, C. Mathis, and S. Lefrant, Phys. Rev. B **64**, 245424 (2001).

[15] T. Pichler, A. Kukovecz, H. Kuzmany, H. Kataura, and Y. Achiba, Phys. Rev. B **67**, 125416 (2003).

[16] L. Kavan, P. Rapta, and L. Dunsch, Chem. Phys. Lett. **328**, 363 (2000).

[17] L. Kavan, P. Rapta, L. Dunsch, M. J. Bronikowski, P. Willis, and R. Smalley, J. Phys. Chem. B **105**, 10764 (2001).

[18] C. P. An, Z. V. Vardeny, Z. Iqbal, J. M. Spinks, R. H. Baughman, and A. Zakhidov, Synth. Met. **116**, 411 (2001).

[19] J. N. Barisci, G. G. Wallace, R. H. Baughman, and L. Dunsch, J. Electroanal. Chem. **488**, 92 (2000).
[20] M. Stoll, P. M. Rafailov, W. Frenzel, and C. Thomsen, Chem. Phys. Lett. **375**, 625 (2003).
[21] S. Gupta, M. Hughes, A. H. Windle, and J. Robertson, J. Appl. Phys. **95**, 2038 (2004).
[22] P. Corio, P. S. Santos, V. W. Brar, G. G. Samsonidze, S. G. Chou, and M. S. Dresselhaus, Chem. Phys. Lett. **370**, 675 (2003).
[23] O. Dubay, G. Kresse, and H. Kuzmany, Phys. Rev. Lett. **88**, 235506 (2002).
[24] H. Kataura, Y. Kumazawa, Y. Maniwa, Y. Ohtsuka, R. Sen, S. Suzuki, and Y. Achiba, Carbon **38**, 1691 (2000).
[25] H. Shimoda, B. Gao, X. P. Tang, A. Kleinhammes, L. Fleming, Y. Wu, and O. Zhou, Phys. Rev. Lett. **88**, 015502 (2002).
[26] P. M. Rafailov, M. Stoll, J. Maultzsch, and C. Thomsen, in *Electronic Properties of Novel Materials-Molecular Nanostructures* edited by H. Kuzmany, J. Fink, M. Mehring, and S. Roth (2004), AIP, New York, p. 153.
[27] P. M. Rafailov, M. Stoll, and C. Thomsen, J. Phys. Chem. B **108**, 19241 (2004).
[28] J. Choi, I. A. Samayoa, S.-C. Lim, C. Jo, Y. C. Choi, Y. H. Lee, and P. A. Dowben, Phys. Lett. A **299**, 601 (2002).
[29] C. Jo, C. Kim, and Y. H. Lee, Phys. Rev. B **65**, 035420 (2002).
[30] L. Kavan, L. Dunsch, and H. Kataura, Chem. Phys. Lett. **361**, 79 (2002).
[31] U. Dettlaff-Weglikowska, V. Skakalova, R. Graupner, S. H. Jhang, B. H. Kim, H. J. Lee, L. Ley, Y. W. P. S. Berber, D. Tomanek, and S. Roth, J. Am. Chem. Soc. **127**, 5125 (2005).
[32] In using the notations LO or TO we mean phonons with a vibrational pattern predominantly along the nanotube axis or circumference, respectively. Note that purely axial and circumferential vibrations can exist only in achiral nanotubes.
[33] J. Maultzsch, S. Reich, U. Schlecht, and C. Thomsen, Phys. Rev. Lett. **91**, 087402 (2003).
[34] J. Maultzsch, S. Reich, and C. Thomsen, Phys. Rev. B **65**, 233402 (2002).
[35] E. Unger, A. Graham, F. Kreupl, M. Liebau, and W. Hoenlein, Curr. Appl. Phys. **2**, 107 (2002).